Environmental Science and Pollution Research (2021) 28:2342–2354
https://doi.org/10.1007/s11356-020-10635-0

RESEARCH ARTICLE

Application of seed residues from *Anadenanthera macrocarpa* and *Cedrela fissilis* as alternative adsorbents for remarkable removal of methylene blue dye in aqueous solutions

Yamil L. O. de Salomón[1] · Jordana Georgin[1] · Dison S. P. Franco[2] · Matias Schadeck Netto[2] · Edson Luiz Foletto[2] · Daniel Allasia[1] · Guilherme Luiz Dotto[2]

Received: 16 June 2020 / Accepted: 25 August 2020 / Published online: 3 September 2020

Abstract

Two novel ecological and low-cost adsorbents were prepared from seed residues of the tree species *Anadenanthera macrocarpa* and *Cedrela fissilis* for the removal of methylene blue dye in water. The materials were comminuted and characterized by different techniques. The particles of samples have a rough surface with cavities. The optimum dosage and pH for both materials were 1 g L^{-1} and pH 8. The pseudo-second-order model was the most suitable for describing the adsorption kinetics for both systems. The *Anadenanthera macrocarpa* presented a maximum experimental capacity of 228 mg g^{-1}, while the *Cedrela fissilis*, a similar capacity of 230 mg g^{-1} at 328 K. The Tóth model was proper for describing the equilibrium curves for both systems. The thermodynamic indicators show that the adsorption process is spontaneous and endothermic for both materials. The application of materials for the simulated effluent treatment showed 74 and 78% of color removal using *Anadenanthera macrocarpa* and *Cedrela fissilis* samples, respectively. Overall, seed residues of *Anadenanthera macrocarpa* and *Cedrela fissilis* could be potentially applied for adsorptive removal of colored contaminants in wastewater.

Keywords Adsorption · Seed residue · *Anadenanthera macrocarpa* · *Cedrela fissilis* · Methylene blue

Introduction

The dyes are often used in the textile, leather, cosmetic, plastic, pharmaceuticals, and food process industries (Garg et al. 2004). The discharges from these industries carry a series of intermediate dyes, which generate large volumes of effluents with different degrees of toxicity (Bhatti et al. 2020). In this way, the colored pollutants are becoming common at hydric bodies, and thus a major preoccupation with the ecosystems (Baig et al. 2019; Wekoye et al. 2020). The methylene blue is the most common dye for its category, which is used in the dyeing process of the cotton and silk (Hameed et al. 2007). In addition to the environmental problems, the strident exposition to the MB causes several health injuries (Vadivelan and Kumar 2005).

Several technologies have been employed for the removal of colored contaminants in water, and among them, the adsorption has been found to be a promising option (Asif et al., 2016) due to applicability at different scenarios, easy implementation, the requirement of less space, and satisfactory cost-benefit when they aligned to efficient adsorbents (Bonilla-Petriciolet et al. 2017; Salleh et al. 2011; Shakoor and Nasar 2018; Rafatullah et al. 2010; Li et al. 2018).

In the literature, it is possible to find the application and development of different adsorbents for the removal of several pollutants. For instance, chitin biochar has been employed for the removal of phenol and 2-nitrophenol (Li et al. 2019a). *Annona crassiflora* seeds were employed as adsorbents for the removal of crystal violet dye (Franco

Responsible Editor: Tito Roberto Cadaval Jr

Electronic supplementary material The online version of this article (https://doi.org/10.1007/s11356-020-10635-0) contains supplementary material, which is available to authorized users.

✉ Guilherme Luiz Dotto
guilherme_dotto@yahoo.com.br

[1] Sanitary and Environmental Engineering Department, Federal University of Santa Maria, Santa Maria 97105-900, Brazil

[2] Chemical Engineering Department, Federal University of Santa Maria-UFSM, Roraima Avenue 1000, Santa Maria, RS 97105-900, Brazil

Table 1 Chemical composition and concentration of the simulated textile effluent

Dyes and compounds	Concentration (mg L^{-1})	λ_{max} (nm)
Methylene blue	100	664
Crystal violet	50	586
Malachite green	50	615
Sodium chloride (NaCl)	100	–
Sodium carbonate (Na_2CO_3)	100	–
pH	9.1	–

et al. 2020), while the *Azadirachta indica* was used to remove Cu^{2+} and Pb^{+2} ions in water (Costa et al. 2020). Chitosan/polyamide nanofibers have been used for the removal of Reactive Black 5 and Ponceau 4R (Li et al. 2019b). Brazilian berry seeds (*Eugenia uniflora*) (Georgin et al. 2020a) and psyllium seeds (Malakootian and Heidari 2018) were applied for adsorption of methylene blue and reactive orange 16, respectively. Besides, the application of carbon nanotubes in single and binary mixtures for the adsorption of rhodamine B and crystal violet (Li et al. 2020a) was studied. *Morgina stenopetala* seeds were used as adsorbents of Cd^{2+}, Pb^{2+}, and Cu^{2+} (Kebede et al. 2018), whereas black cumin (*Nigella sativa* L.) was used for adsorption of methylene blue (Siddiqui et al. 2018). The application of ashitaba waste and walnut shell–based activated carbon for the adsorption of Congo red and methylene blue was also verified (Li et al. 2020b). Last, papaya seeds were applied as potential adsorbents for the removal of different types of pollutants in water (Weber et al. 2013; Paz et al. 2013; Foletto et al. 2013; Weber et al. 2014). Although there are many studies concerning the employment of different seed-based

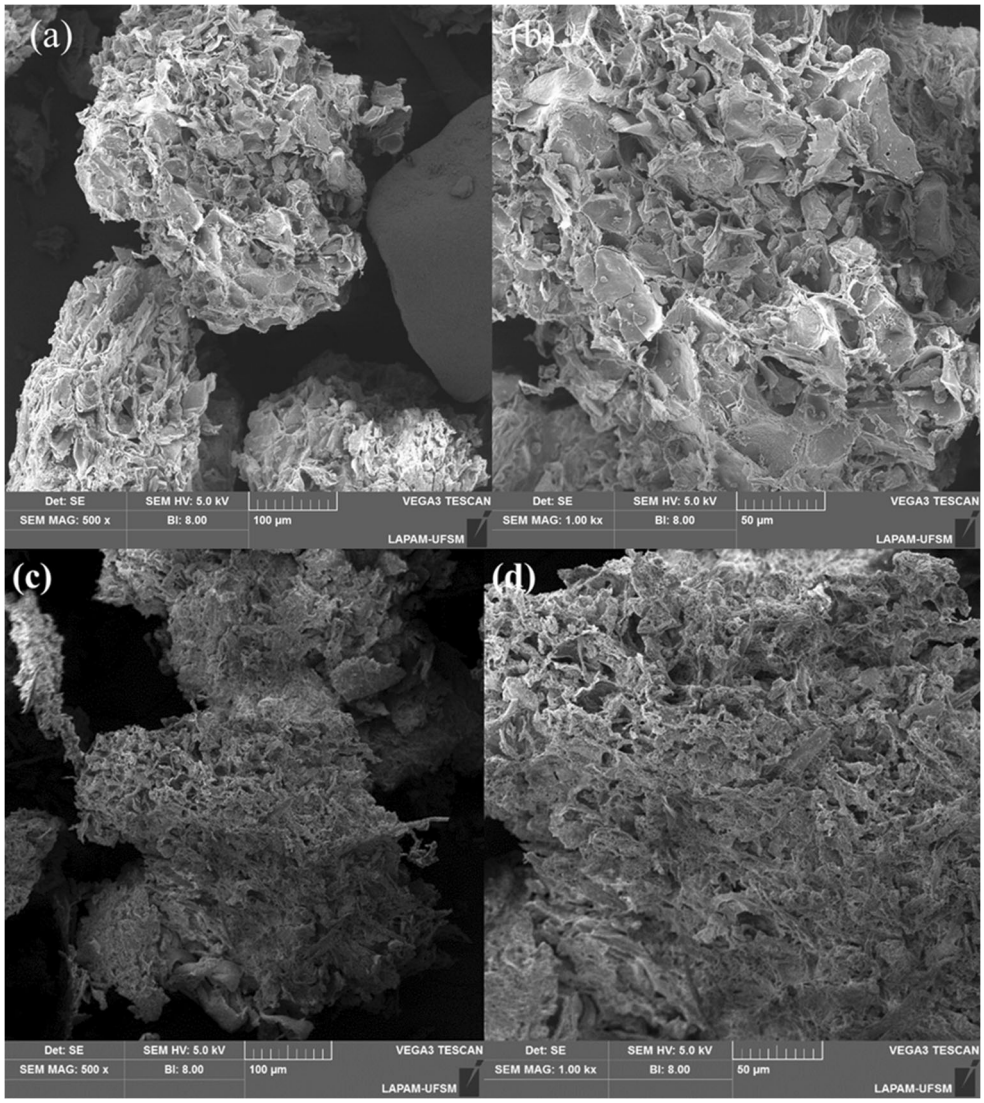

Fig. 1 SEM images for the RASP (**a**, **b**) and CASP (**c**, **d**), with magnifications of × 200 and × 5000

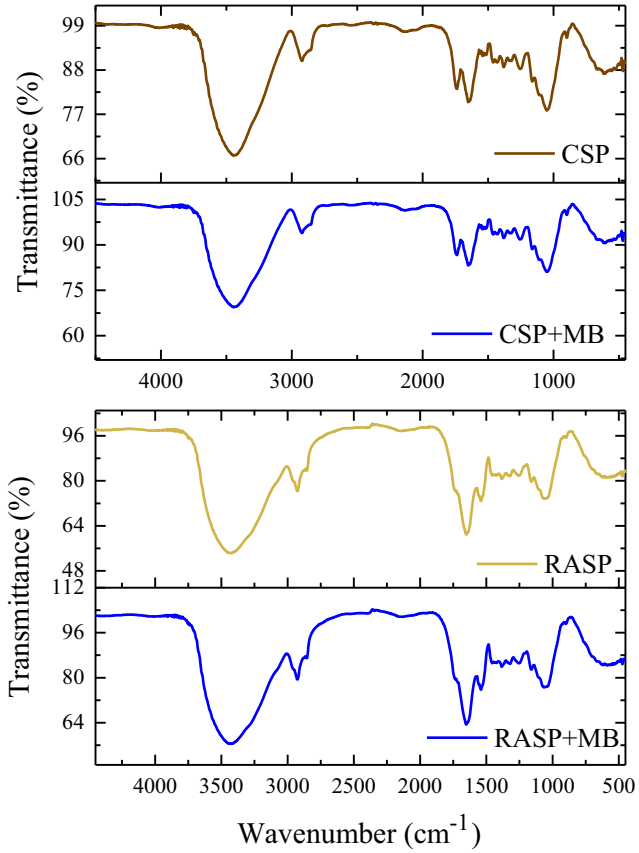

Fig. 2 FT-IR spectra and respective identified bands of RASP and CSP samples

adsorbents, no work using seed residues of *Anadenanthera macrocarpa* and *Cedrela fissilis* has been reported so far.

The *Anadenanthera macrocarpa* is a tree species native to Brazil, belonging to the *Fabaceae* family, popularly known as red angico. Rich in tannins, its bark is indicated in folk medicine for the treatment of respiratory diseases, inflammatory processes, and healing (Figueredo et al. 2013). Another forest species native to Brazil and of great occurrence in South America is *Cedrela fissilis*, popularly known as pink cedar, belonging to the *Meliaceae* family. Its wood is considered noble, with high commercial value, due to this species has been suffering in the last years with illegal deforestation for later commercialization (Muellner et al. 2009; Muellner et al. 2010). Both forest species have peculiarly shaped fruits, with a woody aspect and brown color. Besides, they open at certain times of the year releasing the seeds present in their internal structure, and then fall to the soil, without having other uses, becoming waste (Pennington et al. 2004; Siqueira-Silva et al. 2016).

This work aimed to investigate the potential application of seed residues from *Anadenanthera macrocarpa* and *Cedrela fissilis* as adsorbents for the removal of methylene blue in the water. The physical and chemical properties of materials were determined by different characterization techniques. The adsorption assays were conducted at optimum experimental conditions, and kinetic and equilibrium experiments were developed. Besides, the adsorbents were also applied for color removal from simulated textile effluent.

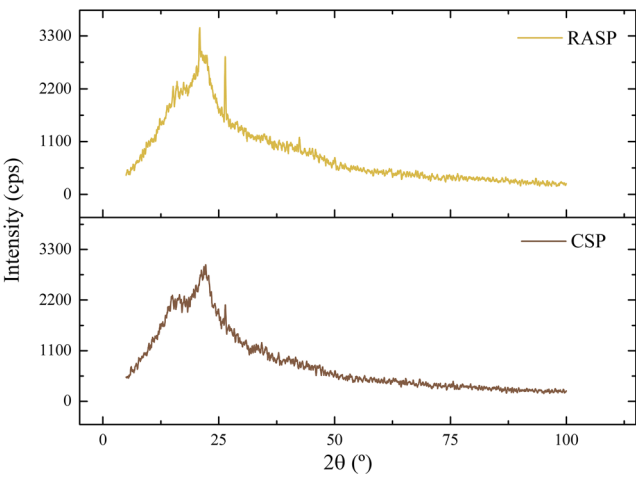

Fig. 3 XRD patterns of RASP and CSP samples

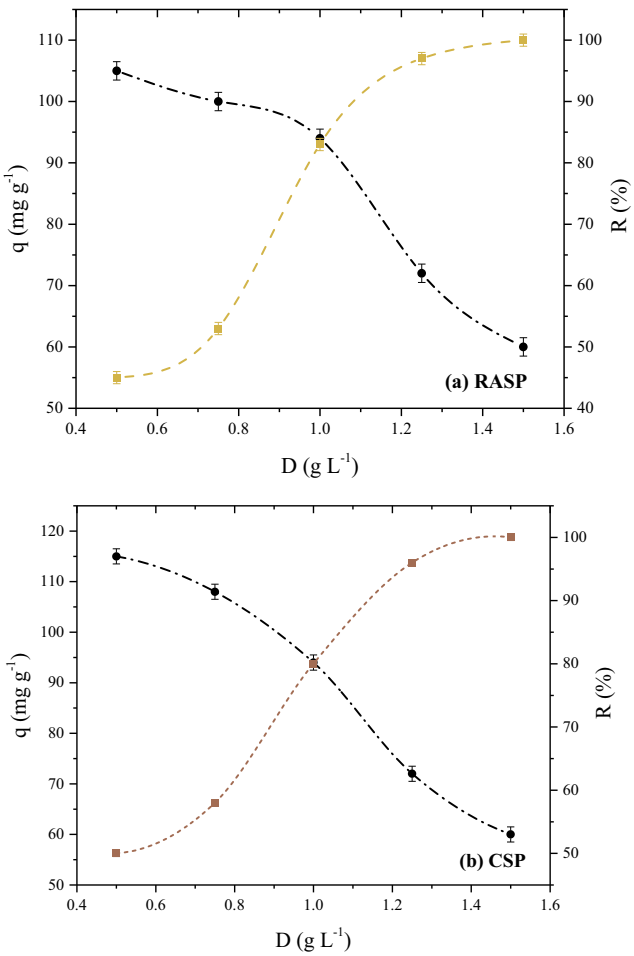

Fig. 4 Dosage effect for the adsorption of MB onto **a** RASP and **b** CSP samples

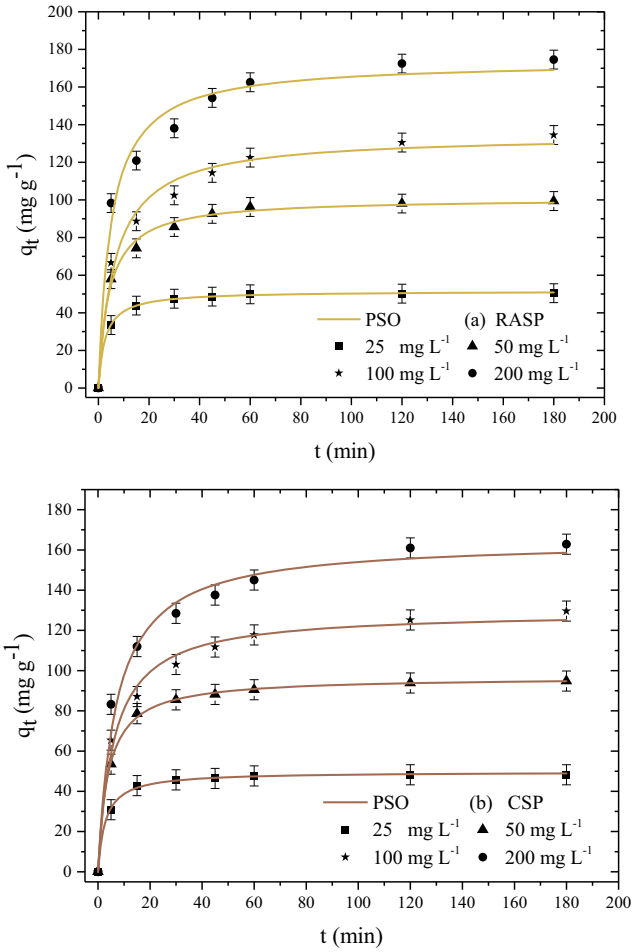

Fig. 5 Kinetic curves for the adsorption of MB onto **a** RASP and **b** CSP samples

Materials and methods

Chemicals and solution preparation

Methylene blue (MB) (molecular formula: $C_{16}H_{18}C1N_3S$, molecular weight: 319.87 g mol^{-1}, dimensions: 14.3 Å wide, 6.1 Å depth, 4 Å thick, and molecular volume of 241.9 cm^3 mol^{-1}) was obtained from Sigma-Aldrich. The MB solutions were prepared using deionized water, according to the desired experimental condition. The pH solution was measured using a Digimed apparatus (DM 20, Brazil). All the adsorption experiments were conducted by a thermostatic agitator (Marconi, MA 093, Brazil) at 150 rpm.

Preparation of adsorbents

The seed residues of *Anadenanthera macrocarpa* and *Cedrela fissilis* were collected in the forest at the Federal University of Santa Maria (Brazil). The seeds were dried at 50 °C for 24 h and then comminuted employing a knife grinder (Marconi, MA 340, Brazil) and further dried at 50 °C for 3 h. After, the particles were sieved by a 60-mesh sieve, obtaining particles with a diameter inferior to 250 μm. Both adsorbents presented a brown color, as shown in Fig. S1. The powders were stored in vacuum bags and labeled as RASP (red angico seed powder) and CSP (cedar seed powder).

Adsorbent characterization

It is essential to investigate the adsorbent properties, such as the morphology, functional groups, and crystallographic structure. For the morphological analysis, a scanning electron microscopy (SEM, Tescan - Vega 3SB, Czech Republic) was employed, operating at 10 kV. The identification of the major functional groups for RASP and CSP samples before and after the adsorption was carried out by a Fourier transform infrared spectrophotometer (FT-IR, Shimadzu, Prestige-21, Japan). In this analysis, 35 mg of each adsorbent was pressed with dried analytical potassium bromate. X-ray diffraction (XRD) was used to investigate the structure of the samples (Rigaku, Miniflex 300, Japan).

Batch adsorption experiments

The adsorption assays were conducted to investigate the dosage effect, kinetic, and equilibrium profile. The dosage effect was analyzed using 0.5 to 1.5 g L^{-1}. For this, the adsorbent (RASP or CSP) was put in contact with 50 mL of MB solution (initial concentration of 100 mg L^{-1}). The mixtures were agitated during 180 min at 298 K. The kinetic experiments were realized using the optimum dosage, at the initial concentrations of 25, 50, 100, and 200 mg L^{-1}. Similarly, the adsorbent was added to 50 mL of MB solution at 298 K. The samples were collected at 0, 5, 15, 30, 45, 60, 120, and 180 min. Last, the equilibrium experiments were obtained at 298, 308, 318, and 328 K, with initial concentrations of 50, 100, 150, 200, and 300 mg L^{-1}. The adsorbents were mixed with 50 mL of MB solution and agitated for 5 h to ensure the equilibrium.

The detection of the MB concentration in the liquid phase was done by employing a UV-vis spectrophotometer (Shimadzu, UV mini 1240, Japan), operating at 664 nm. All tests were realized in triplicate ($n = 3$), and the blank test was also carried out to guarantee the data reproducibility. All samples were separated by centrifugation (Centribio, 80-2B, Brazil) at 4000 rpm for 20 min. The percentage of dye removal, adsorption capacity at any time, and equilibrium were used to evaluate the adsorption process.

Kinetic, isotherm, and thermodynamic models

The adsorption kinetics of MB dye on the adsorbents was analyzed according to the Elovich (Elovich and Larinov 1962), pseudo-second-order (Ho and Mckay 1999), pseudo-first-order (Lagergren 1898), and general order models (Liu

Table 2 Kinetic parameters estimated for the adsorption of MB onto RASP adsorbent

Model	MB initial concentration (mg L^{-1})			
	50	100	150	200
Pseudo-first order				
q_1 (mg g^{-1})	48.86	93.54	122.15	159.33
k_1 (min^{-1})	0.2171	0.1554	0.1067	0.1414
R^2	0.9914	0.9659	0.9409	0.9369
R^2_{adj}	0.9760	0.9061	0.8395	0.8288
ARE (%)	3.05	6.98	10.05	9.86
MSE (mg g^{-1})^2	3.00	45.02	136.66	246.66
Pseudo-second order				
q_2 (mg g^{-1})	51.52	100.81	134.42	173.65
k_2 (g mg^{-1} min^{-1})	7.28×10^{-3}	2.33×10^{-3}	1.13×10^{-3}	1.15×10^{-3}
R^2	0.9998	0.9946	0.9857	0.9826
R^2_{adj}	0.9994	0.9848	0.9603	0.9516
ARE (%)	0.44	2.72	5.04	5.20
MSE (mg g^{-1})^2	0.07	7.17	33.06	68.17
General order				
q_n (mg g^{-1})	50.42	99.40	134.48	174.57
k_n (min^{-1} (g mg^{-1})$^{n-1}$)	1.88×10^{-2}	2.58×10^{-3}	4.85×10^{-4}	3.48×10^{-4}
n (-)	1.73	1.99	2.20	2.27
R^2	0.9998	0.9946	0.9857	0.9826
R^2_{adj}	0.9992	0.9810	0.9503	0.9395
ARE (%)	0.56	3.01	4.64	4.68
MSE (mg g^{-1})^2	0.13	9.64	34.90	69.11
Elovich				
a (g mg^{-1})	3117.82	401.08	119.35	344.04
b (mg g^{-1} min^{-1})	0.2202	0.0830	0.0503	0.0437
R^2	0.9828	0.9880	0.9955	0.9946
R^2_{adj}	0.9522	0.9665	0.9874	0.9849
ARE (%)	4.90	3.88	2.17	2.35
MSE (mg g^{-1})^2	6.01	15.88	10.43	21.06

and Shen 2008) (equations shown in Supplementary material (S.2)). For the adsorption isotherms, Langmuir (Langmuir 1918), Freundlich (Freundlich 1906), and Tóth (Tóth 2002) models were chosen (Equations are shown in Supplementary material (S.3)). The thermodynamic calculations were based on the methodology proposed by Lima et al. (2019), whose equations are shown in Supplementary material (S.4). The fit quality evaluation is shown in Supplementary material (S.5). The model parameters were estimated through script programming on Matlab 2017.

Preparation of synthetic textile effluent

Some studies report the preparation of synthetic wastewater containing textile dyes, from the mixture of dye with a source of water, and chemicals. The mixture aims to combine the residual features with the particularities of the actual effluents, which contains several chemicals, auxiliaries, and dyes added during the textile production process (Yaseen and Scholz 2018). Thus, a simulated effluent was prepared to verify the capacity of angico and cedar samples for the treatment of residual effluents containing organic pollutants and salinity (Table 1). For each test, 4.5 g L^{-1} of adsorbent was added in 100 mL of simulated effluent solution and stirred at 200 rpm for 4 h under room temperature (298 K). The dosage of 4.5 g L^{-1} was applied in this work due to the unsatisfactory results obtained by the using dosage equal to 1 g L^{-1}, as observed in preliminary tests realized by our research group (Georgin et al. 2020c). Then, absorbance scans of the solution were performed before and after adsorption tests, at a wavelength of 200 to 800 nm, using the UV-Vis spectrophotometer (Shimadzu, UV-2600, Japan). The color removal was determined by the ratio between the area of the curves using the Matlab 2017 with trapz function.

Table 3 Kinetic parameters estimated for the adsorption of MB onto CSP adsorbent

Model	MB initial concentration (mg L^{-1})			
	50	100	150	200
Pseudo-first order				
q_1 (mg g^{-1})	47.00	90.28	117.98	148.94
k_1 (min^{-1})	0.2042	0.1650	0.1154	0.1047
R^2	0.9949	0.9892	0.9509	0.9579
R^2_{adj}	0.9859	0.9700	0.8659	0.8847
ARE (%)	2.52	3.77	9.02	8.66
MSE (mg $g^{-1})^2$	1.63	13.21	105.36	146.32
Pseudo-second order				
q_2 (mg g^{-1})	49.65	96.76	129.30	164.66
k_2 (g mg^{-1} min^{-1})	7.04×10^{-3}	2.64×10^{-3}	1.28×10^{-3}	8.77×10^{-4}
R^2	0.9987	0.9993	0.9904	0.9933
R^2_{adj}	0.9963	0.9981	0.9732	0.9814
ARE (%)	1.25	0.81	4.02	3.37
MSE (mg $g^{-1})^2$	0.42	0.83	20.65	23.15
Pseudo-general order				
q_n (mg g^{-1})	48.24	94.83	129.60	162.88
k_n (min^{-1}(g $mg^{-1})^{n-1}$)	2.87×10^{-2}	6.42×10^{-3}	5.85×10^{-4}	7.01×10^{-4}
n (-)	1.58	1.79	2.18	2.06
R^2	0.9987	0.9993	0.9904	0.9933
R^2_{adj}	0.9954	0.9976	0.9665	0.9768
ARE (%)	0.60	0.93	3.62	2.96
MSE (mg $g^{-1})^2$	0.13	1.02	21.08	28.26
Elovich				
a (g mg^{-1})	2060.43	592.56	145.25	123.66
b (mg g^{-1} min^{-1})	0.2208	0.0916	0.0542	0.0400
R^2	0.9763	0.9783	0.9952	0.9936
R^2_{adj}	0.9343	0.9398	0.9867	0.9823
ARE (%)	5.76	5.80	2.62	3.35
MSE (mg $g^{-1})^2$	7.70	26.60	10.23	22.09

Results and discussion

Characteristics of RASP and CSP samples

The SEM images with different magnifications of RASP and CSP samples are shown in Fig. 1. The surface of the RASP sample is highly rugous, irregular, and heterogeneous, with the presence of empty spaces smaller than 10 μm (Fig. 1a, b). Likewise, the CSP sample exhibits irregularities on its morphology, with a rough surface containing cavities. It is of interest that the materials presented such characteristics, since these empty spaces and channels may positively favor the adsorption (Georgin et al. 2018a, b). Similar characteristics were found in other lignocellulosic materials such as Pará chestnut husk (Georgin et al. 2018a, b), Araticum (*Annona crassiflora*) seeds (Franco et al. 2020), and golden trumpet tree bark (Hernandes et al. 2019).

Figure 2 shows the FT-IR spectra of RASP and CSP samples. The forest wood (seeds, wood, leaves) are lignocellulosic materials mainly constituted of three groups: lignin, cellulose, and hemicellulose (Salleh et al. 2011). In the case of the RASP and CSP samples, the following bands were identified: the high stretch at 3434 cm^{-1} is associated with the presence of OH (Saha et al. 2012; Feng et al. 2011); the band deformation at 2917 cm^{-1} is attributed to the C–H bond (alkyl, aliphatic and aromatic groups); at 1731 cm^{-1}, on the CPS sample, can be found a C=O bond (Babalola et al. 2016); band at 1664 cm^{-1} can be related to C=O and N–H bonds, belonging to the amide (Kumar and Ahmad 2011); the RASP sample presents a 1535 cm^{-1} minor band related to the C=O (ketone or carbonyl) (Chakraborty et al. 2011). Last, the bands at 1050 and 605 cm^{-1} are related to C–OH, C–O–C, and aromatic bonds (Román et al. 2013). From Fig. 2, it was found that after the adsorption, the transmittance increased for both adsorbents. In

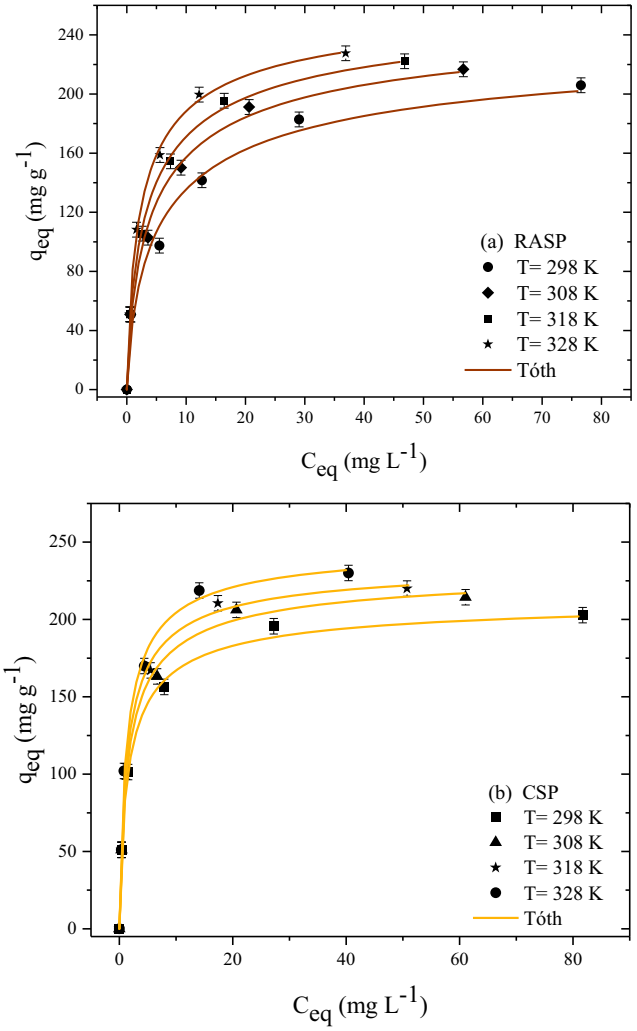

Fig. 6 Equilibrium curves for the biosorption of MB onto **a** RASP and **b** CSP samples

this case, the formation/absence of bands was not found in comparison with the original adsorbent samples. The general increase of the transmittance suggests that the main functional groups of the material are involved in the adsorption mechanism. Groups such as O–H and CO may be involved in the adsorption; this is related to their negative nature, leading to interact with positively charged MB molecules (Guo et al. 2020; Pang et al. 2019).

The XRD patterns for the RASP and CSP samples are shown in Fig. 3. Both materials exhibit a broad peak, with a maximum at 26.39 and 22.19° for the RASP and CSP samples, respectively. The wide peaks from 10° to 30° can be attributed to the lignin content (Georgin et al. 2020b). It is known that an adsorbent with amorphous characteristics has a more disorganized structure and larger void spaces, and these characteristics contribute to the adsorption of dye molecules (Georgin et al. 2020b). Similar behaviors were observed by the XRD analysis of the bark of *Moringa oleifera* (Reddy et al. 2011).

Table 4 Equilibrium parameters estimated for the adsorption of MB onto RASP adsorbent

Temperature (K)				
Model	298	308	318	328
Langmuir				
q_{mL} (mg g^{-1})	218.46	227.25	231.00	233.80
k_L (L mg^{-1})	0.1660	0.2503	0.3314	0.4835
R^2	0.9722	0.9840	0.9899	0.9936
R^2_{adj}	0.9537	0.9733	0.9832	0.9894
ARE (%)	13.73	10.80	8.27	5.53
MSE (mg g^{-1})^2	216.64	139.33	92.52	61.59
Freundlich				
k_F ((mg g^{-1})(mg L^{-1})$^{-1/nF}$)	205.92	216.75	222.16	227.57
$1/n_F$ (dimensionless)	0.2256	0.3091	0.3877	0.5321
R^2	0.9798	0.9761	0.9721	0.9644
R^2_{adj}	0.9664	0.9601	0.9535	0.9406
ARE (%)	9.46	11.22	12.43	15.05
MSE (mg g^{-1})^2	157.33	208.11	256.09	344.13
Tóth				
q_{mT} (mg g^{-1})	247.11	260.10	266.59	267.73
k_T (L mg^{-1})	0.5803	0.6513	0.7263	0.8393
n_T (dimensionless)	0.5991	0.6209	0.6300	0.6592
R^2	0.9860	0.9943	0.9979	0.9986
R^2_{adj}	0.9650	0.9857	0.9947	0.9965
ARE (%)	9.69	6.37	3.70	2.29
MSE (mg g^{-1})^2	145.59	66.27	26.04	17.84

pH justification and adsorbent dosage effect

The pH plays an important role in the adsorption process of the dye molecules since it controls the electrostatic force intensity of charges transmitted by dye molecules (Mahmoud et al. 2012). In this study, all tests were performed at the natural pH of the MB solution (pH = 8). Several studies prove that the pH around 8 is ideal for MB removal in water (Franciski et al. 2018; Netto et al. 2019), and the explanation is that at low pH, there is a strong repulsion between the positively charged dye ions and the negatively charged adsorbent surface, due to protonation of the functional groups present on the surface, resulting in low efficiency in MB removal. The reverse process occurs with an increase in pH value, causing a greater increase in removal efficiency due to deprotonation of the groups that are positively charged on the adsorbent surface, plus the electrostatic forces that attract the negatively charged places in the biosorbent and the dye cations (Saha et al. 2012).

The adsorbent dosage (D) used to remove the dye is also important for determining the adsorption capacity (q) given the initial concentration of the dye in solution (Singh et al.

Table 5 Equilibrium parameters estimated for the adsorption of MB onto CSP adsorbent

Temperature (K)				
Model	298	308	318	328
Langmuir				
q_{mL} (mg g^{-1})	199.50	214.57	221.47	233.08
k_L (L mg^{-1})	0.6716	0.7192	0.7827	0.8333
R^2	0.9925	0.9923	0.9942	0.9935
R^2_{adj}	0.9875	0.9872	0.9904	0.9892
ARE (%)	5.64	5.30	4.08	4.48
MSE (mg $g^{-1})^2$	60.99	72.32	57.23	70.45
Freundlich				
k_F ((mg g^{-1})(mg $L^{-1})^{-1/nF}$)	198.16	214.38	220.02	230.06
$1/n_F$ (dimensionless)	0.6939	0.7218	0.7975	0.8656
R^2	0.9444	0.9498	0.9467	0.9455
R^2_{adj}	0.9073	0.9163	0.9112	0.9092
ARE (%)	16.82	17.05	18.00	18.96
MSE (mg $g^{-1})^2$	453.42	472.59	529.01	590.67
Tóth				
q_{mT} (mg g^{-1})	215.40	235.27	238.16	249.91
k_T (L mg^{-1})	1.0824	1.1118	1.1200	1.1390
n_T (dimensionless)	0.6855	0.6745	0.7289	0.7473
R^2	0.9975	0.9974	0.9965	0.9961
R^2_{adj}	0.9937	0.9935	0.9930	0.9901
ARE (%)	1.93	3.06	3.72	5.42
MSE (mg $g^{-1})^2$	27.50	32.69	33.55	57.02

2017). For both materials, it was found a typical tendency; i.e., the increase of the adsorbent dosage decreased the adsorption capacity and increased the removal percentage, as shown in Fig. 4. In the case of the RAPS sample, the adsorption capacity decreases from 105 to 60 mg g^{-1} with a removal percentage ranging from 55 to 100%. The values for the CPS sample trend 115 to 54 mg g^{-1} with the removal of 55 to 100%. It is possible to consider that 1 g L^{-1} is the optimum condition for the adsorption (intersection of the curves). A similar trend was observed by Jain and Gogate (2018) by using *Prunus Dulci* bark activated to remove the Acid Green 25 dye.

Adsorption kinetics and fitted models

The kinetic data for both systems with different initial concentrations (25, 50, 100, and 200 mg L^{-1}) are shown in Fig. 5. The first aspect to be noticed is that the initial concentration influenced the inclination of the adsorption data. About the equilibrium time for both systems, it is reached at approximately 60 min. However, for the cases where the C_0 is 25 mg L^{-1}, the equilibrium time is reached at 30 min. For the adsorption capacities, the RASP sample reached 174.57 mg g^{-1}, and the CSP sample reached 162.88 mg g^{-1} in the higher initial concentration (200 mg L^{-1}). The behavior of adsorption kinetics is due to the higher adsorption rate that occurs in the first minutes. At this moment, the surface of the material possesses more adsorption empty sites. As time increases, the adsorption rate decreases as well since the adsorption site is more occupied and reaching the equilibrium. A similar kinetic profile was also observed by Aichour and Zaghouane-Boudiaf (2019), using composites of modified citrus peel based on cellulose and calcium alginate for the removal of cationic dyes Gentian violet and methylene blue.

The estimated parameters for the kinetic models related to RASP and CSP samples are shown in Tables 2 and 3, respectively. From all the evaluated models, the pseudo-second-order model was the most suitable for describing both systems. For the RASP sample, the pseudo-second-order model resulted in an $R^2_{adj} \geq 0.9516$ and $MSE \leq 68.17$ (mg $g^{-1})^2$, while the CSP sample achieved $R^2_{adj} \geq 0.9732$ and $MSE \leq 23.15$ (mg $g^{-1})^2$. Moreover, the pseudo-second-order model was also able to predict the adsorption capacity for all cases and both systems. Kinetic adjustments for the pseudo-second-order model have also been found in the adsorption of orange solimax dye onto malt bagasse (Fontana et al. 2016), adsorption of tartrazine dye onto wood industry residues (Banerjee and Chattopadhyaya 2013), and on the adsorption of Orange G dye by modified *Pyracantha coccínea* (Gorgulu and Celik 2013).

Adsorption isotherm and thermodynamic estimation

The adsorption equilibrium for the MB adsorption onto RASP and CSP samples is shown in Fig. 6. At first observation, both systems show increasing value for the adsorption capacities with the rise of the temperature. For the RASP sample, the equilibrium adsorption capacity change from 205.92 to 227.57 mg g^{-1}. The CSP sample shows a similar trend with a slight increase of 202.78 to 230.06 mg g^{-1}. This indicates an endothermic nature for both the systems. In the adsorption process, the temperature has two important effects. The increase in temperature decreases the viscosity of the solution, which increases the diffusion rate of adsorbate molecules through the outer boundary layer and within the pores of adsorbent particles, thus increasing the adsorption sites, and consequently increasing the adsorption capacity (Al-Qodah 2000; Nandi et al. 2009; Wekoye et al. 2020).

The computed parameters for the isotherm models are presented in Tables 4 and 5. For both cases, the Tóth model shows better conformity for describing the experimental data. The goodness of fit shows $R^2_{adj} \geq 0.965$ and $MSE \leq 145.59$ (mg $g^{-1})^2$ for the RASP and $R^2_{adj} \geq 0.990$ and $MSE \leq 57.02$ (mg $g^{-1})^2$ for CSP. The Tóth model is an expansion of the

Table 6 Comparison of RASP and CSP adsorbents with other adsorbents employed for the removal of MB

Adsorbent	pH	T(K)	q_{max} (mg g^{-1})	Isotherm model	References
PCS	8	328	230.06	Tóth	This study
RASP	8	328	227.57	Tóth	This study
Date stones	7.0	303	398.19	Sips	Ahmed and Dhedan 2012
Mesoporous Iraqi red kaolin	8.0	303	240.4	Langmuir	Jawad and Abdulhameed 2020
Golden trumpet tree bark (*Handroanthus albus*)	10	328	232.25	Langmuir	Hernandes et al. 2019
Silica gel supported calix arene cage	12	293	212.77	Langmuir	Temel et al. 2020
Carbonized watermelon (*Citrullus lanatus*) rind	5.4	303	200	Langmuir	Jawad et al. 2019
Brazilian berry seeds (*Eugenia uniflora*)	8.0	328	189.6	Langmuir	Georgin et al. 2020a
Carboxymethyl cellulose/carboxylated graphene oxide composite microbeads	10.0	328	180.32	Langmuir	Eltaweil et al. 2018
Walnut shells powder	6.8	293	178.9	Langmuir	Miyah et al. 2018
Porous activated kaolinite	6.0	296	171.0	Langmuir	Asuha et al. 2019
EDTA-modified bentonite	5.4	303	160	Langmuir	Castro et al. 2018
Garlic peel	6.0	323	142.86	Langmuir	Hameed and Ahmad 2009
Nano-Fe_3O_4/carboxyl-functionalized baker's yeast composites	6.0	308	141.75	Langmuir	Du et al. 2017
Carbon nanotubes	4.0	310	132.61	Sips	Sharyari et al. 2010
Biocomposite films	6.9	308	103.66	Langmuir	Somsesta et al. 2019
Chestnut husk (Bertholletia excelsa)	4.0	328	83.8	Freundlich	Georgin et al. 2018a, b
Acid washed black cumin seed power	7.0	300	73.52	Langmuir	Siddiqui et al. 2018
Tartaric acid treated bagasse	9.0	313	65.79	Langmuir	Low et al. 2012
Salix babylonica (weeping willow)	7	23C	60.97	Langmuir	Khodabandehloo et al. 2017
Kaolinite	6.0	296	45.6	Langmuir	Asuha et al. 2019
Canola	7	328	11.25	Sips	Balarak et al. 2015

Langmuir model, that considerate multi-layer adsorption and the heterogeneous surface of the materials (Wu et al. 2013). Thus, the model suggests that the MB adsorption process onto the RASP and CSP adsorbents may be heterogeneous. The Tóth model was able to describe other liquid systems, such as adsorption of nickel(II) onto biochar derived from the walnut shell (Georgieva et al. 2020). Another key thing to remember, this model has the greatest affinity to surfaces with non-uniform distribution of the active sites, leading to random adsorption in several layers (Chandra and Chattopadhyay 2019).

A comparison among adsorption capacities of RASP and CSP samples with other adsorbents reported in the literature for MB removal is presented in Table 6. The results reveal that the samples prepared in this work have remarkable adsorptive performances for MB in aqueous solution. Therefore, these residues become alternative adsorbents for the removal of dyes from aqueous solutions, assuming the following advantages: abundance and easy availability in nature, and thus being ecological.

The thermodynamic computed values are presented in Table 7. The equilibrium constant (K_e) was estimated from the Tóth isotherm. It was found that the adsorption process is spontaneous, with ΔG^0 ranging from − 30.07 to − 34.10 kJ mol^{-1} for the RASP sample and − 31.61 to − 34.93 kJ mol^{-1} for the CSP sample. The ΔH^0 for both systems was found 9.87 kJ mol^{-1} (RASP) and 1.30 kJ mol^{-1} (CSP), indicating an endothermic behavior, which corroborates the isotherm profile for both systems. Last, the ΔS^0 is related to the adjustments of the molecules on the material surface and, in this

Table 7 Thermodynamics parameters for the RASP/MB and CSP/MB systems

Adsorbent	T (K)	K_e (-)	ΔG^0 (kJ mol^{-1})	ΔH^0 (kJ mol^{-1})	ΔS^0 (kJ mol^{-1} K^{-1})
RASP	298	185609.0	− 30.07	9.87	0.1339
	308	208318.3	− 31.37		
	318	232307.1	− 32.68		
	328	268450.1	− 34.10		
CSP	298	346215.5	− 31.61	1.31	0.1105
	308	355610.3	− 32.74		
	318	358232.0	− 33.82		
	328	364309.2	− 34.93		

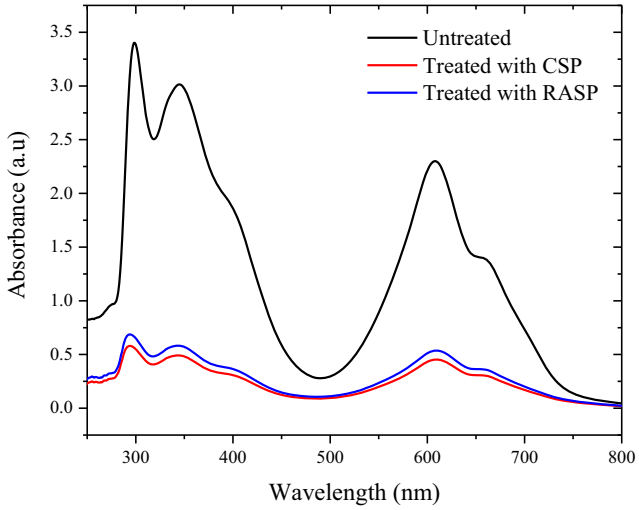

Fig. 7 UV-Vis absorption spectra before and after the effluent treatment with RASP and CSP samples

work, the values were 0.133 and 0.11 kJ mol^{-1} K^{-1} for the RASP and CSP samples, respectively.

Color removal from simulated textile effluent

In general, the adsorption studies in the batch system are focused on the removal of a single compound. However, this work investigated the application of the RASP and CSP samples for the color removal of simulated effluent (Table 1). The UV-Vis absorption spectra for the effluents before and after the application of the RASP and CSP samples are shown in Fig. 7. From the areas under the curves, it is possible to estimate that the RASP sample was able to remove 74.58% of color, and the CSP sample, 78.54%. According to the results observed in the UV region, it is possible to infer that there was the formation of other compounds due to the breaking of the covalent bonds present on the dye molecule, which are simultaneously removed by the adsorbents.

Conclusion

The residue-based adsorbents investigated in this work (*Anadenanthera macrocarpa* and *Cedrela fissilis*) were effective in the removal of methylene blue dye in water. From the characterization techniques, it was possible to find chemical groups typical of lignocellulosic materials. Both materials had a rough, highly heterogeneous surface with the presence of particles with varying shapes and sizes. The dosage of 1 g L^{-1} of RAPS and CSP was enough to remove 80% and 83% of the MB dye. The adsorption kinetics for both materials achieved the equilibrium time at 60 min when the concentration was higher than 50 mg L^{-1}. The pseudo-second-order model was the most suitable for describing the adsorption kinetics. From the equilibrium experiments, it was found that the *Anadenanthera macrocarpa* presented a maximum equilibrium capacity of 228 mg g^{-1} and *Cedrela fissilis*, a similar capacity of 230 mg g^{-1} at 328 K. The Tóth model is the most proper one for describing the isotherm data for both systems and indicates that the adsorption can occur in multi-layer and/or the surface of the RASP and CASP is heterogeneous. In the treatment of the simulated effluent containing different dyes, the materials showed an excellent decolorization performance, removing 74% for the RASP sample and 78% for the CSP sample. Therefore, the seed wastes of angico and cedar become alternative adsorbents for the treatment of textile effluents, presenting as advantages the low cost and the efficiency in removing dyes from aqueous solutions.

References

Ahmed MJ, Dhedan SK (2012) Equilibrium isotherms and kinetics modeling of methylene blue adsorption on agricultural wastes-based activated carbons. Fluid Phase Equilib 317:9–14. https://doi.org/10.1016/j.fluid.2011.12.026

Aichour A, Zaghouane-Boudiaf H (2019) Single and competitive adsorption studies of two cationic dyes from aqueous mediums onto cellulose-based modified citrus peels/calcium alginate composite. Int J Biol Macromol 154:1227–1236. https://doi.org/10.1016/j.ijbiomac.2019.10.277

Al-Qodah Z (2000) Adsorption of dyes using shale oil ash. Water Res 34(17):4295–4303. https://doi.org/10.1016/s0043-1354(00)00196-2

Asif TM, Bhatt HN, Iqbal M (2016) Solar red and brittle blue direct dyes adsorption onto Eucalyptus angophoroides bark: equilibrium, kinetics and thermodynamic studies. J Environ Chem Eng 4(2):2431–2439. https://doi.org/10.1016/j.jece.2016.04.020

Asuha S, Fei F, Wurendaodi W, Zhao S, Wu H, Zhuang X (2019) Activation of kaolinite by a low-temperature chemical method and its effect on methylene blue adsorption. Powder Technol 361:624–632. https://doi.org/10.1016/j.powtec.2019.11.068

Babalola JO, Koiki BA, Eniayewu Y, Salimonu A, Olowoyo JO, Oninla VO, Omorogie MO (2016) Adsorption efficacy of Cedrela odorata seed waste for dyes: non linear fractal kinetics and non linear equilibrium studies. J Environ Chem Eng 4(3):3527–3536. https://doi.org/10.1016/j.jece.2016.07.027

Baig U, Uddin MK, Gondal MA (2019) Removal of hazardous azo dye from water using synthetic nano adsorbent: facile synthesis, characterization, adsorption, regeneration and design of experiments. Coll Surf A: Physicochem Eng Aspects 124031:124031. https://doi.org/10.1016/j.colsurfa.2019.124031

Balarak D, Jaafari J, Hassani G, Mahdavi Y, Tyagi I, Agarwal S, Gupta VK (2015) The use of low-cost adsorbent (Canola residues) for the adsorption of methylene blue from aqueous solution: isotherm, kinetic and thermodynamic studies. Coll Interf Sci Commun 7:16–19. https://doi.org/10.1016/j.colcom.2015.11.004

Banerjee S, Chattopadhyaya MC (2013) Adsorption characteristics for the removal of a toxic dye, tartrazine from aqueous solutions by a low cost agricultural by-product. Arab J Chem 10:S1629–S1638. https://doi.org/10.1016/j.arabjc.2013.06.005

Bhatti HN, Safa Y, Yakout SM, Shair OH, Iqbal M, Nazir A (2020) Efficient removal of dyes using carboxymethyl cellulose/alginate/polyvinyl alcohol/rice husk composite: adsorption/desorption,

kinetics and recycling studies. Int J Biol Macromol 150:861–870. https://doi.org/10.1016/j.ijbiomac.2020.02.093

Bonilla-Petriciolet A, Mendoza-Castillo DI, Reynel-Ávila HE (2017) Adsorption processes for water treatment and purification. Springer International Publishing, Berlin, Germany

Castro MLFA, Abad MLB, Sumalinog DAG, Abarca RRM, Paoprasert P, de Luna MDG (2018) Adsorption of methylene blue dye and Cu(II) ions on EDTA-modified bentonite: isotherm, kinetic and thermodynamic studies. Sustain Environ Res 28:197–205. https://doi.org/10.1016/j.serj.2018.04.001

Chakraborty S, Chowdhury S, Das Saha P (2011) Adsorption of crystal violet from aqueous solution onto NaOH-modified rice husk. Carbohydrate Pol 86(4):1533–1541. https://doi.org/10.1016/j.carbpol.2011.06.058

Chandra A, Chattopadhyay S (2019) Chain length and acidity of carboxylic acids influencing adsorption/desorption mechanism and kinetics over anion exchange membrane. Coll Surf A: Physicochem Eng Aspects 124395:124395. https://doi.org/10.1016/j.colsurfa.2019.124395

Costa WD, da Silva Bento AM, de Araújo JAS, Menezes JMC, da Costa JGM, da Cunha FAB, Pereira TRN (2020) Removal of copper (II) ions and lead (II) from aqueous solutions using seeds of Azadirachta indica A. Juss as bioadsorvent Environ Res 109213:109213. https://doi.org/10.1016/j.envres.2020.109213

Du Z, Zhang Y, Li Z, Chen H, Wang Y, Wang G, Zhang Y (2017) Facile one-pot fabrication of nano-Fe_3O_4/carboxyl-functionalized baker's yeast composites and their application in methylene blue dye adsorption. Appl Surf Sci 392:312–320. https://doi.org/10.1016/j.apsusc.2016.09.050

Elovich SY, Larinov OG (1962) Theory of adsorption from solutions of non-electrolytes on solid (I) equation adsorption from solutions and the analysis of its simplest form, (II) verification of the equation of adsorption isotherm from solutions.

Eltaweil AS, Elgarhy GS, El-Subruiti GM, Omer AM (2018) Novel carboxymethyl cellulose/carboxylated graphene oxide composite microbeads for efficient adsorption of cationic methylene blue dye. Int J Biol Macromol 154:307–318. https://doi.org/10.1016/j.ijbiomac.2020.03.122

Feng N, Guo X, Liang S, Zhu Y, Liu J (2011) Biosorption of heavy metals from aqueous solutions by chemically modified orange peel. J Hazard Mater 185(1):49–54. https://doi.org/10.1016/j.jhazmat.2010.08.114

Figueredo FG, Ferreira EO, Lucena BFF, Torres CMG, Lucetti DL, Lucetti ECP, Matias EFF (2013) Modulation of the antibiotic activity by extracts from Amburana cearensis A. C. Smith andAnadenanthera macrocarpa (Benth.) Brenan. Biomed Res Int 1-5. https://doi.org/10.1155/2013/640682

Foletto EL, Weber CT, Bertuol DA, Mazutti MA (2013) Application of papaya seeds as a macro-/mesoporous biosorbent for the removal of large pollutant molecule from aqueous solution: equilibrium, kinetic, and mechanism studies. Sep Sci Technol 48:2817–2824. https://doi.org/10.1080/01496395.2013.808213

Fontana KB, Chaves ES, Sanchez JDS, Watanabe ERLR, Pietrobelli JMTA, Lenzi GG (2016) Textile dye removal from aqueous solutions by malt bagasse: isotherm, kinetic and thermodynamic studies. Ecotox Environ Safety 124:329–336. https://doi.org/10.1016/j.ecoenv.2015.11.012

Franciski MA, Peres EC, Godinho M, Perondi D, Foletto EL, Collazzo GC, Dotto GL (2018) Development of CO_2 activated biochar from solid wastes of a beer industry and its application for methylene blue adsorption. Waste Manag 78:630–638. https://doi.org/10.1016/j.wasman.2018.06.040

Franco DSP, Georgin J, Drumm FC, Netto MS, Allasia D, Oliveira MLS, Dotto GL (2020) Araticum (Annona crassiflora) seed powder (ASP) for the treatment of colored effluents by biosorption. Environ Sci Pollut Res 27:11184–11194. https://doi.org/10.1007/s11356-019-07490-z

Freundlich HMF (1906) Over the adsorption in solution. J Phys Chem 57:385–471

Garg V, Kumar R, Gupta R (2004) Removal of malachite green dye from aqueous solution by adsorption using agro-industry waste: a case study of Prosopis cineraria. Dyes Pigments 62(1):1–10. https://doi.org/10.1016/j.dyepig.2003.10.016

Georgieva VG, Gonsalvesh L, Tavlieva MP (2020) Thermodynamics and kinetics of the removal of nickel (II) ions from aqueous solutions by biochar adsorbent made from agro-waste walnut shells. J Mol Liq 112788:112788. https://doi.org/10.1016/j.molliq.2020.112788

Georgin J, da Silva MB, da Silveira SJ, Foletto EL, Allasia D, Dotto GL (2018a) Removal of Procion Red dye from colored effluents using H_2SO_4-/HNO_3-treated avocado shells (Persea americana) as adsorbent. Environ Sci Pollut Res 25(7):6429–6442. https://doi.org/10.1007/s11356-017-0975-1

Georgin J, Marques BS, Peres EC, Allasia D, Dotto GL (2018b) Biosorption of cationic dyes by Pará chestnut husk (Bertholletia excelsa). Water Sci Technol 77(6):1612–1621. https://doi.org/10.2166/wst.2018.041

Georgin J, Franco DSP, Netto MS, Allasia D, Oliveira MLS, Dotto GL (2020a) Treatment of water containing methylene by biosorption using Brazilian berry seeds (Eugenia uniflora). Environ Sci Pollut Res 27(17):20831–20843. https://doi.org/10.1007/s11356-020-08496-8

Georgin J, Franco D, Drumm FC, Grassi P, Netto MS, Allasia D, Dotto GL (2020b) Powdered biosorbent from the mandacaru cactus (Cereus jamacaru) for discontinuous and continuous removal of Basic Fuchsin from aqueous solutions. Powder Technol 364:584–592. https://doi.org/10.1016/j.powtec.2020.01.064

Georgin J, Franco D, Netto MS, Allasia D, Oliveira MLS, Dotto GL (2020c) Evaluation of Ocotea puberula bark powder (OPBP) as an effective adsorbent to uptake crystal violet from colored effluents: alternative kinetic approaches. Environ Sci Pollut Res 27:25727–25739. https://doi.org/10.1007/s11356-020-08854-6

Gorgulu Ari A, Celik S (2013) Biosorption potential of Orange G dye by modified Pyracantha coccinea: batch and dynamic flow system applications. Chem Eng J 226:263–270. https://doi.org/10.1016/j.cej.2013.04.073

Guo D, Li Y, Cui B, Hu M, Luo S, Ji B, Liu Y (2020) Natural adsorption of methylene blue by waste fallen leaves of Magnoliaceae and its repeated thermal regeneration for reuse. J Clean Prod 267:121903. https://doi.org/10.1016/j.jclepro.2020.121903

Hameed BH, Ahmad AA (2009) Batch adsorption of methylene blue from aqueous solution by garlic peel, an agricultural waste biomass. J Hazard Mater 164(2-3):870–875. https://doi.org/10.1016/j.jhazmat.2008.08.084

Hameed BH, Ahmad AL, Latiff KNA (2007) Adsorption of basic dye (methylene blue) onto activated carbon prepared from rattan sawdust. Dyes Pigments 75(1):143–149. https://doi.org/10.1016/j.dyepig.2006.05.039

Hernandes PT, Oliveira MLS, Georgin J, Franco DSP, Allasia D, Dotto GL (2019) Adsorptive decontamination of wastewater containing methylene blue dye using golden trumpet tree bark (*Handroanthus albus*). Environ Sci Pollut Res 26:31924–31933. https://doi.org/10.1007/s11356-019-06353-x

Ho YS, McKay G (1999) Pseudo-second order model for sorption processes. Process Biochem **34**(5):451–465

Jain SN, Gogate PR (2018) Efficient removal of Acid Green 25 dye from wastewater using activated Prunus Dulcis as biosorbent: batch and column studies. J Environ Manag 210:226–238. https://doi.org/10.1016/j.jenvman.2018.01.008

Jawad AH, Abdulhameed AS (2020) Mesoporous Iraqi red kaolin clay as an efficient adsorbent for methylene blue dye: adsorption kinetic,

isotherm and mechanism study. Surf Interf 18:100422. https://doi.org/10.1016/j.surfin.2019.100422

Jawad AH, Razuan R, Appaturi JN, Wilson LD (2019) Adsorption and mechanism study for methylene blue dye removal with carbonized watermelon (Citrullus lanatus) rind prepared via one-step liquid phase H_2SO_4 activation. Surf Interf 16:76–84. https://doi.org/10.1016/j.surfin.2019.04.012

Kebede TG, Mengistie AA, Dube S, Nkambule TTI, Nindi MM (2018) Study on adsorption of some common metal ions present in industrial effluents by Moringa stenopetala seed powder. J Environ Chem Eng 6(1):1378–1389. https://doi.org/10.1016/j.jece.2018.01.012

Khodabandehloo A, Rahbar-Kelishami A, Shayesteh H (2017) Methylene blue removal using Salix babylonica (Weeping willow) leaves powder as a low-cost biosorbent in batch mode: kinetic, equilibrium, and thermodynamic studies. J Mol Liq 244:540–548. https://doi.org/10.1016/j.molliq.2017.08.108

Kumar R, Ahmad R (2011) Biosorption of hazardous crystal violet dye from aqueous solution onto treated ginger waste (TGW). Desalination 265(1-3):112–118. https://doi.org/10.1016/j.desal.2010.07.040

Lagergren S (1898) Zur Theorie der Sogenannten Adsorption Gelöster Stoffe. Kung Svenska Vetenskap 24:1–39

Langmuir I (1918) The adsorption of gases on plane surfaces of glass, mica and platinum. J Amer Chem Soc 40:1361–1403

Li Z, Hanafy H, Zhang L, Sellaoui L, Netto MS, Oliveira MLS, Seliem MK, Dotto GL, Bonilla-Petriciolet A, Li Q (2020b) Adsorption of congo red and methylene blue dyes on an ashitaba waste and a walnut shell-based activated carbon from aqueous solutions: experiments, characterization and physical interpretations. Chem Eng J 388:124263. https://doi.org/10.1016/j.cej.2020.124263

Li Z, Sellaoui L, Dotto GL, Ben Lamine A, Bonilla-Petriciolet A, Hanafy H, Belmabrouk H, Netto MS, Erto A (2019b) Interpretation of the adsorption mechanism of Reactive Black 5 and Ponceau 4R dyes on chitosan/polyamide nanofibers via advanced statistical physics model. J Mol Liq 285:165–170. https://doi.org/10.1016/j.molliq.2019.04.091

Li Z, Sellaoui L, Dotto GL, Bonilla-Petriciolet A, Ben Lamine A (2019a) Understanding the adsorption mechanism of phenol and 2-nitrophenol on a biopolymer-based biochar in single and binary systems via advanced modeling analysis. Chem Eng J 371:1–6. https://doi.org/10.1016/j.cej.2019.04.035

Li Z, Sellaoui L, Franco DSP, Netto MS, Georgin J, Dotto GL, Bajahzar A, Belmabrouk A, Bonilla-Petriciolet A, Li Q (2020a) Adsorption of hazardous dyes on functionalized multiwalled carbon nanotubes in single and binary systems: experimental study and physicochemical interpretation of the adsorption mechanism. Chem Eng J 389:124467. https://doi.org/10.1016/j.cej.2020.124467

Li Z, Wang G, Zhai K, He C, Li Q, Guo P (2018) Methylene blue adsorption from aqueous solution by loofah sponge-based porous carbons. Colloids Surf A: Physicochem Eng Aspects 538:28–35. https://doi.org/10.1016/j.colsurfa.2017.10.046

Lima EC, Hosseini-Bandegharaei A, Moreno-Piraján JC, Anastopoulos I (2019) A critical review of the estimation of the thermodynamic parameters on adsorption equilibria. Wrong use of equilibrium constant in the Van't Hoof equation for calculation of thermodynamic parameters of adsorption. J Mol Liq 273:425–434. https://doi.org/10.1016/j.molliq.2018.10.048

Liu Y, Shen L (2008) A general rate law equation for biosorption. Biochem Eng J 38:390–394

Low LW, Teng TT, Morad N, Azahari B (2012) Studies on the adsorption of methylene blue dye from aqueous solution onto low-cost tartaric acid treated bagasse. APCBEE Procedia 1:103–109. https://doi.org/10.1016/j.apcbee.2012.03.018

Mahmoud DK, Salleh MAM, Karim WAWA, Idris A, Abidin ZZ (2012) Batch adsorption of basic dye using acid treated kenaf fibre char: equilibrium, kinetic and thermodynamic studies. Chem Eng J 181-182:449–457. https://doi.org/10.1016/j.cej.2011.11.116

Malakootian M, Heidari MR (2018) Reactive orange 16 dye adsorption from aqueous solutions by psyllium seed powder as a low-cost biosorbent: kinetic and equilibrium studies. Appl Water Sci 8:212. https://doi.org/10.1007/s13201-018-0851-2

Miyah Y, Lahrichi A, Idrissi M, Khalil A, Zerrouq F (2018) Adsorption of methylene blue dye from aqueous solutions onto walnut shells powder: equilibrium and kinetic studies. Surf Interf 11:74–81. https://doi.org/10.1016/j.surfin.2018.03.006

Muellner AN, Pennington TD, Chase MW (2009) Molecular phylogenetics of Neotropical Cedreleae (mahogany family, Meliaceae) based on nuclear and plastid DNA sequences reveal multiple origins of "Cedrela odorata.". Molec Phylogenb Evolut 52(2):461–469. https://doi.org/10.1016/j.ympev.2009.03.025

Muellner AN, Pennington TD, Koecke AV, Renner SS (2010) Biogeography of Cedrela (Meliaceae, Sapindales) in Central and South America. American J Botany 97(3):511–518. https://doi.org/10.3732/ajb.0900229

Nandi BK, Goswami A, Purkait MK (2009) Adsorption characteristics of brilliant green dye on kaolin. J Hazard Mater 161(1):387–395. https://doi.org/10.1016/j.jhazmat.2008.03.110

Netto MS, da Silva NF, Mallmann ES, Dotto GL, Foletto EL (2019) Effect of salinity on the adsorption behavior of methylene blue onto comminuted raw avocado residue: CCD-RSM Design. Water Air Soil Pollut 230:187. https://doi.org/10.1007/s11270-019-4230-x

Pang X, Sellaoui L, Franco DSP, Netto MS, Georgin J, Dotto GL, Abu Shayeb MK, Belmabrouk H, Bonilla-Petriciolet A, Li Z (2019) Preparation and characterization of a novel mountain soursop seeds powder adsorbent and its application for the removal of crystal violet and methylene blue from aqueous solutions. Chem Eng J 391:123617. https://doi.org/10.1016/j.cej.2019.123617

Paz DS, Baiotto A, Schwaab M, Mazutti MA, Bassaco MM, Bertuol D, Foletto EL, Meili L (2013) Use of papaya seeds as a biosorbent of methylene blue from aqueous solution. Water Sci Technol 68(2):441–447. https://doi.org/10.2166/wst.2013.185

Pennington RT, Lavi M, Prado DE, Pendry CA, Pell SK, Butterworth CA (2004) Historical climate change and speciation: neotropical seasonally dry forest plants show patterns of both Tertiary and Quaternary diversification. Philosop Trans the Royal Soc B: Biolog Sci 359(1443):515–538. https://doi.org/10.1098/rstb.2003.1435

Rafatullah M, Sulaiman O, Hashim R, Ahmad A (2010) Adsorption of methylene blue on low-cost adsorbents: a review. J Hazard Mater 177(1-3):70–80. https://doi.org/10.1016/j.jhazmat.2009.12.047

Reddy DHK, Ramana DKV, Seshaiah K, Reddy AVR (2011) Biosorption of Ni(II) from aqueous phase by Moringa oleifera bark, a low cost biosorbent. Desalination 268(1-3):150–157. https://doi.org/10.1016/j.desal.2010.10.011

Román S, Valente Nabais JM, Ledesma B, González JF, Laginhas C, Titirici MM (2013) Production of low-cost adsorbents with tunable surface chemistry by conjunction of hydrothermal carbonization and activation processes. Microporous Mesoporous Mater 165:127–133. https://doi.org/10.1016/j.micromeso.2012.08.006

Saha PD, Chakraborty S, Chowdhury S (2012) Batch and continuous (fixed-bed column) biosorption of crystal violet by Artocarpus heterophyllus (jackfruit) leaf powder. Colloids Surf B: Biointerfaces 92:262–270. https://doi.org/10.1016/j.colsurfb.2011.11.057

Salleh MAM, Mahmoud DK, Karim WAWA, Idris A (2011) Cationic and anionic dye adsorption by agricultural solid wastes: a comprehensive review. Desalination 280(1-3):1–13. https://doi.org/10.1016/j.desal.2011.07.019

Shakoor S, Nasar A (2018) Adsorptive decontamination of synthetic wastewater containing crystal violet dye by employing Terminalia arjuna sawdust waste. Groundw Sustain Dev 7:30–38. https://doi.org/10.1016/j.gsd.2018.03.004

Sharyari Z, Goharrizi AS, Azadi M (2010) Experimental study of methylene blue adsorption from aqueous solutions onto carbon nano tubes. Int J Water Res Environ Eng 2(2):16–28. https://doi.org/10.5897/IJWREE

Siddiqui SI, Rathi G, Chaudhry SA (2018) Acid washed black cumin seed powder preparation for adsorption of methylene blue dye from aqueous solution: thermodynamic, kinetic and isotherm studies. J Mol Liq 264:275–284. https://doi.org/10.1016/j.molliq.2018.05.065

Singh H, Chauhan G, Jain AK, Sharma SK (2017) Adsorptive potential of agricultural wastes for removal of dyes from aqueous solutions. J Environ Chem Eng 5(1):122–135. https://doi.org/10.1016/j.jece.2016.11.030

Siqueira-Silva AI, Pereira EG, Modolo LV, Lemos-Filho JP, Paiva EAS (2016) Impact of cement dust pollution on Cedrela fissilis Vell. (Meliaceae): a potential bioindicator species. Chemosphere 158:56–65. https://doi.org/10.1016/j.chemosphere.2016.05.047

Somsesta N, Sricharoenchaikul V, Aht-Ong D (2019) Adsorption removal of methylene blue onto activated carbon/cellulose biocomposite films: equilibrium and kinetic studies. Mater Chem Phys 240:122221. https://doi.org/10.1016/j.matchemphys.2019.122221

Temel F, Turkyilmaz M, Kucukcongar S (2020) Removal of methylene blue from aqueous solutions by silica gel supported calix[4]arene cage: investigation of adsorption properties. European Pol J 125:109540. https://doi.org/10.1016/j.eurpolymj.2020.109540

Tóth J (2002) Adsorption. theory, modelling, and analysis, Dekker, New York.

Vadivelan V, Kumar KV (2005) Equilibrium, kinetics, mechanism, and process design for the sorption of methylene blue onto rice husk. J Colloid Interface Sci 286(1):90–100. https://doi.org/10.1016/j.jcis.2005.01.007

Weber CT, Foletto EL, Meili L (2013) Removal of tannery dye from aqueous solution using papaya seed as an efficient natural biosorbent. Water Air Soil Pollut 224:1427. https://doi.org/10.1007/s11270-012-1427-7

Weber CT, Collazzo G, Mazutti MA, Foletto EL, Dotto GL (2014) Removal of hazardous pharmaceutical dyes by adsorption onto papaya seeds. Water Sci Technol 70(1):102–107. https://doi.org/10.2166/wst.2014.200

Wekoye JN, Wanyonyi WC, Wangila PT, Tonui M (2020) Kinetic and equilibrium studies of Congo red dye adsorption on cabbage waste powder. Environ Chem Ecotoxicol 2:24–31. https://doi.org/10.1016/j.enceco.2020.01.004

Wu KT, Wu PH, Wu FC, Jreng RL, Juang RS (2013) A novel approach to characterizing liquid-phase adsorption on highly porous activated carbons using the Toth equation. Chem Eng J 221:373–381. https://doi.org/10.1016/j.cej.2013.02.012

Yaseen DA, Scholz M (2018) Textile dye wastewater characteristics and constituents of synthetic effluents: a critical review. Int J Environ Sci Technol 16:1193–1226. https://doi.org/10.1007/s13762-018-2130-z